PROGRESS IN TIME-SERIES SOIL MOISTURE RETRIEVAL USING L- AND S-BAND RADAR BACKSCATTER

Dustin Horton[1], Alexandra Bringer[1], Joel T. Johnson[1], Jeonghwan Park[2,3], Rajat Bindlish[3]

[1]Department of Electrical and Computer Engineering and ElectroScience Laboratory,
The Ohio State University, Columbus, OH Horton.378@osu.edu
[2]Global Science & Technology, Inc., Greenbelt, MD 20770
[3]NASA Goddard Space Flight Center, Greenbelt, MD

ABSTRACT

L- and S-band observations from NASA's Passive/Active L/S band (PALS) sensor from the SMEX02 campaign were used to estimate soil moisture. The retrieval process is based on the "alpha approximation" method. This method utilizes a time-series of normalized radar backscatter measurements as well as ancillary information to estimate soil moisture over the Walnut Creek watershed. The resulting retrieved soil moistures are compared to in-situ soil moisture measurements at multiple test sites within the watershed. The calculations show reasonable results for both L- and S-band and provide further insight into the use of L- and S-bands for the upcoming NASA/ISRO mission.

Index Terms—**Soil moisture, L-band, S-band, SMEX02, radar, PALS.**

1. INTRODUCTION

Surface soil moisture has been shown to be a key climatic component in the Earth's hydrological cycle. It plays an important role in the terrestrial hydrology to study the water cycle [1-6]. Soil moisture also impacts the evapotranspiration cycle and has a strong influence over weather patterns [4, 6-7]. Better knowledge of soil moisture can therefore improve our understanding of these relationships and weather forecasts. Relationships between infiltration and surface water runoff [4] further show that soil moisture impacts flood dynamics, so improved soil moisture measurements can lead to better flood prediction models and management of water resources [8]. Knowledge of soil moisture is also crucial under drought conditions in order to support irrigation planning and predict potential drought impacts [9].

Given these applications, it is important to develop accurate soil moisture remote sensing methods at desirable spatial and temporal resolutions over large geographic areas [10]. Airborne or spaceborne radar measurements provide one approach for remotely sensing soil moisture. While many investigations have been conducted using X-, C-, and L-band radar backscatter, few references have considered soil moisture remote sensing using S-band radar [11]. This paper will investigate further the use of S-band for soil moisture retrieval through the application of a time-series soil moisture retrieval method using L- and S-band radar measurements taken from the PALS instrument during the SMEX02 campaign. The investigation and comparison of L- and S-band retrievals also provides further insight into the use of both frequencies in anticipation of the NASA/ISRO SAR mission (NISAR) [12].

2. METHODOLOGY

2.1 Retrieval Method

While many radar soil moisture retrieval algorithms have been proposed, these past approaches require the use of complicated forward scattering models and ancillary knowledge of vegetation properties [14]. To eliminate the need for forward scattering models and vegetation data, the "alpha approximation" method is used for soil moisture retrieval in this paper. A brief review of the method is provided below; a detailed explanation can be found in [13], and simplified explanations can be found in [10] and [14].

In the alpha approximation method, the NRCS from a vegetated scene is represented as:

$$\sigma_{pq}^{t} = \sigma_{pq}^{s} \exp(-\tau) + \sigma_{pq}^{v} + \sigma_{pq}^{sv} \qquad (1)$$

which is a combination of surface scattering (σ_{pq}^{s}), volume scattering (σ_{pq}^{v}), and surface-volume (σ_{pq}^{sv}) interaction terms. The method nominally assumes that the surface scattering term is dominant, and that its contributions can be expressed as a product of independent functions of soil moisture, vegetation attenuation, and surface roughness [14]. Note that a similar argument can be made for the surface-volume interaction term, so that the approach can also retain applicable when the "double-bounce" term is dominant.

Given a sufficiently short temporal difference between radar measurements, it can be assumed that there is minimal

change in the vegetation and surface roughness for a given scene. Therefore, by taking a ratio of consecutive radar measurements, the vegetation attenuation and surface roughness influences are eliminated. This NRCS ratio can then be expressed as:

$$\left| \frac{\sigma_{PP}^{0(t2)}}{\sigma_{PP}^{0(t1)}} \right| \approx \left| \frac{\alpha_{PP}(\varepsilon_r^{(t2)}, \theta_i)}{\alpha_{PP}(\varepsilon_r^{(t1)}, \theta_i)} \right|^2 \qquad (2)$$

Here the alpha coefficients α_{PP} in polarization combination PP are known functions obtained from the small perturbation method [14-16] and are a function of the soil permittivity and incidence angle. NRCS ratios having the form of (2) obtained from multiple passes can then be arranged into a matrix equation and solved for the alpha coefficients. The resulting alpha coefficients are then mapped into soil moistures through a lookup table that relates soil permittivity (and therefore α_{PP}) to soil moisture and soil texture. For this study, the Mironov dielectric mixing model [17] is used.

2.2 Bounding Solutions

Because the method employs N-1 NRCS ratios obtained from a time series of N NRCS measurements in order to retrieve N soil moistures, it is necessary to provide additional ancillary information to complete the solution. Previous studies have provided maximum and minimum α_{PP} values over the time series for this information. These values in some past studies have been obtained from *in-situ* measurements [11]. For this study, maximum and minimum bounds for α_{PP} were calculated using a texture-based regression equation that was derived using *in-situ* data from all field sites in the campaign. These texture-based bounds were then utilized to perform the soil moisture retrievals in what follows.

3. APPLICATION TO SMEX02 DATASET

3.1 SMEX02 Campaign

Testing was conducted using data from the SMEX02 campaign, which was conducted in June-July 2002 over central Iowa, US. Radar measurements were acquired on June 25, June 27, July 2, and July 5–8 using the PALS instrument [19] over the Walnut Creek watershed. The PALS instrument was flown on a C130 aircraft with a constant incidence angle of 45 degrees and provided a spatial resolution of approximately 330m x 470m [20].

The watershed contained a total of 33 in-situ field sites consisting of both corn and soybean fields. Of these 33 sites, 30 sites had PALS radar measurements with spatial footprint overlap within individual field site bounds. Shallow surface (0-6cm range) soil moisture measurements were taken at these sites on a total of 12 days during the campaign [21] using the techniques described in [22]. For the purposes of this study, the theta probe measurements with site-specific

calibration were used for validating the soil moisture retrievals. The spatial bounds of each field site are defined using the corner geocoordinates provided by [23] with field sites ranging in size from approximately $0.27 - 1.62$ km^2.

3.2 Retrievals

Soil moisture retrievals were conducted over the watershed using a 400m x 400m grid to approximate the spatial footprint of the PALS instrument. The NRCS time-series included all 7 dates of radar observations. A non-weighted average NRCS for each pixel on a given day in the time-series was calculated by averaging radar measurements (in power) having at least 50% of the observed footprint within the geographic bounds of the pixel. The "alpha approximation" method was then applied to each pixel having 7 days of radar measurements using the texture-based bounds described in Section 2.2. Separate retrievals were performed using either HH and VV polarizations at either L- or S-bands.

3.3 Validation using *In-Situ* observations

To validate the results, retrieved soil moisture values were compared to the *in-situ* soil moisture measurements for each of the 30 previously mentioned field sites. This comparison is accomplished by calculating a weighted average of any 400x400 m grid pixels that overlap each field site on each day that has both in-situ measurements and retrieved soil moistures (June 25, June 27, and July 5-8). A weighting value for a pixel over a field site is calculated by dividing the area of overlap between a specific overlapping pixel and a field site by the total area of pixels overlapping a field site. This value is then multiplied by the soil moisture of that pixel and summed with all weighted values overlapping a field site to result in a weighted soil moisture average. To ensure that the weighted averages are representative of each field site for comparison, only sites having 400 x 400 m grid pixel coverage of 50% or more of the site area are analyzed which results in 150 data points for each frequency and polarization combination.

4. RESULTS

Figure 1 plots retrieved and in-situ soil moisture values for the two polarizations and two frequency combinations (LHH in the far-left plot, LVV in the left middle plot, SHH in the right middle plot, and SVV in the far-right plot). Table 1 provides a statistical summary of the comparison including the root-mean-square error, bias, unbiased root-mean-square error, and correlation.

The results show an unbiased RMSE of 0.0642 or less as well as a correlation of 0.5655 or greater. The smallest unbiased RMSE (0.0569) occurs for LVV, and the highest (0.0642) for LHH. In general, VV polarization outperforms HH for unbiased RMSE as well as correlation for L-band, as should be expected given the greater sensitivity of α_{VV} to soil
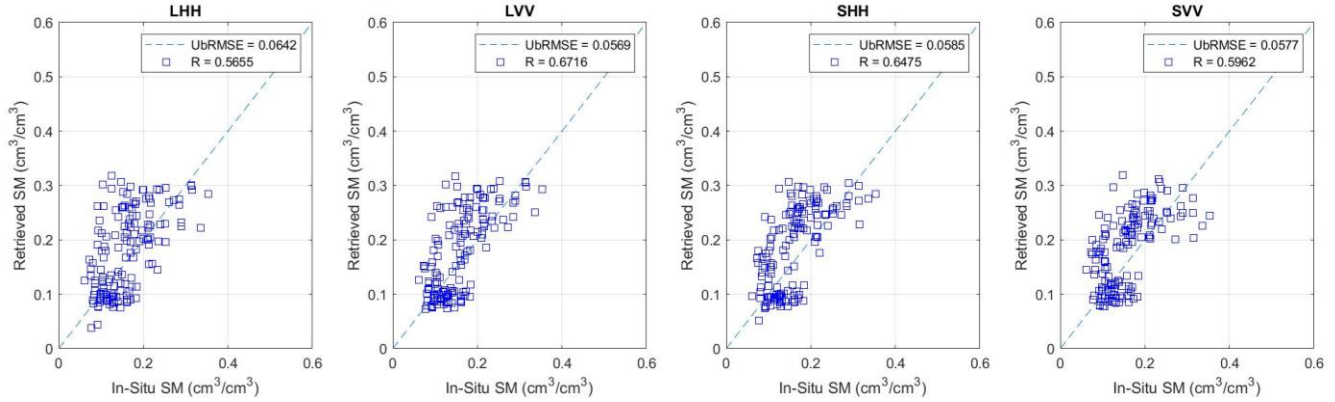
Figure 1. Retrieved vs. *in-situ* soil moisture measurements using a 7-day time-series and texture-based bounds. Left plots represent L-band results, and right plots represent S-band results.

	RMSE	Bias	UBRMSE	Corr.
LHH	0.0671	0.0195	0.0642	0.5655
LVV	0.0601	0.0194	0.0569	0.6716
SHH	0.0634	0.0246	0.0585	0.6475
SVV	0.0630	0.0253	0.0577	0.5962

Table 1. Statistics from the Scatter Plots in Figure 1.

moisture as compared to α_{HH}. While for S-band, VV outperforms HH in unbiased RMSE and HH outperforms VV in correlation. When comparing L- and S-bands, LVV shows a slightly improved UBRMSE as compared to SVV, while SHH in contrast shows a lower UBRMSE than LHH. LVV however shows the highest correlation and lowest unbiased RMSE between retrieved and in-situ soil moistures. Given the relatively small number of observations available from the SMEX02 campaign, the results generally indicate that both L- and S-band radar backscatter data can provide reasonable soil moisture retrievals for the crop conditions considered in SMEX02.

5. CONCLUSIONS

The reported results show reasonable performance for both L- and S-band retrievals using both HH and VV polarizations. These results provide further insight into the use of L- and S-band radar measurements using the alpha approximation method. Additionally, the results show good performance using texture-based information when bounding solutions for the alpha approximation method and provide further insight into alternative bounding options for cases in which *in-situ* information is not available. The results reported further motivate the combined use of L- and S-band radar measurements for use in the upcoming NASA/ISRO NISAR mission and recommend further investigation into a combined frequency soil moisture retrieval method.

6. REFERENCES

[1] Entekhabi, D., E. Njoku, P. O'Neill, K. Kellogg, W. Crow, W. Edelstein, J. Entin, S. Goodman, T. Jackson, J. Johnson, J. Kimball, J. Piepmeier, R. Koster, K. McDonald, M. Moghaddam, S. Moran, R. Reichle, J. C. Shi, M. Spencer, S. Thurman, L. Tsang, J. Van Zyl, "The Soil Moisture Active and Passive (SMAP) Mission," Proceedings of the IEEE, vol. 98, no. 5, 2010.

[2] SMAP Handbook, 2014, document available at: https://smap.jpl.nasa.gov/system/internal_resources/details/original/178_SMAP_Handbook_FINAL_1_JULY_2014_Web.pdf.

[1] P.C. Dubois, J.J. van Zyl, "Measuring soil moisture with imaging radars," IEEE Transactions on Geoscience and Remote Sensing, vol. 33, no. 4, pp. 915-926, 1995.

[2] Srivastava PK, Petropoulos GP, Kerr YH (2016b) Satellite Soil Moisture Retrieval: Techniques and Applications. In: Prashant K Srivastava, George P Petropoulos, Yann H Kerr (eds) Volume I. Elsevier Press, pp 440

[3] Srivastava, P.K. Satellite Soil Moisture: Review of Theory and Applications in Water Resources. *Water Resource Manage* **31,** 3161–3176 (2017). https://doi.org/10.1007/s11269-017-1722-6

[4] T. L. Delworth and S. Manabe, "The influence of potential evaporation on the variabilities of the simulated soil wetness and climate,'' J. Climate, vol. 1, no. 5, pp. 523-547, 1988.

[5] A. K. Betts, J. H Ball, A. C. Baljaars, M. J. Miller, and P. Viterbo, "Coupling between land surface, boundary layer parametrizations and rainfall on local and regional scales: Lessons from the wet summer of 1993," Fifth Con$ Global Change Studies: American Meteor. SOC. Nashville, TN, Jan. 23-28, 1994

[6] Entekhabi, Dara, Ghassem R. Asrar, Alan K. Betts, Keith J. Beven, Rafael L. Bras, Christopher J. Duffy, Thomas Dunne, Randal D. Koster, Dennis P. Lettenmaier, Dennis B. McLaughlin, William J. Shuttleworth, Martinus T. van Genuchten, Ming-Ying Wei, and Eric F. Wood. " An Agenda for Land Surface Hydrology Research and a Call for the Second International Hydrological Decade". *Bulletin of the American Meteorological Society* 80.10